

Enhancing Medical Cross-Modal Hashing Retrieval using Dropout-Voting Mixture-of-Experts Fusion

Jaewon Ahn*
vpersie@yonsei.ac.kr
Graduate School of Integrative
Medicine, Yonsei University
Seoul, South Korea

Woosung Jang*
jwill1994@yonsei.ac.kr
Graduate School of Integrative
Medicine, Yonsei University
Seoul, South Korea

Beakcheol Jang†
bjang@yonsei.ac.kr
Graduate School of Information,
Yonsei University
Seoul, South Korea

Abstract

In recent years, cross-modal retrieval using images and text has become an active area of research, especially in the medical domain. The abundance of data in various modalities in this field has led to a growing importance of cross-modal retrieval for efficient image interpretation, data-driven diagnostic support, and medical education. In the context of the increasing integration of distributed medical data across healthcare facilities with the objective of enhancing interoperability, it is imperative to optimize the performance of retrieval systems in terms of the speed, memory efficiency, and accuracy of the retrieved data. This necessity arises in response to the substantial surge in data volume that characterizes contemporary medical practices. In this study, we propose a novel framework that incorporates dropout voting and mixture-of-experts (MoE) based contrastive fusion modules into a CLIP-based cross-modal hashing retrieval structure. We also propose the application of hybrid loss. So we now call our model MCMFH which is a medical cross-modal fusion hashing retrieval. Our method enables the simultaneous achievement of high accuracy and fast retrieval speed in low-memory environments. The model is demonstrated through experiments on radiological and non-radiological medical datasets.

CCS Concepts

• Applied computing → Life and medical sciences; Health informatics.

Keywords

Cross-Modal Hashing Retrieval, Dropout Voting, Mixture of Experts, Contrastive learning

1 Introduction

In recent years, multimodal retrieval has emerged as a key technology in various fields such as e-commerce, social media, law, and healthcare. In particular, in the medical field, multimodal data retrieval technology is becoming more important as diagnosis and decision-making are based on various types of data such as images, text, and test results. Medical data is characterized by large volumes, multiple modalities, and unstructured data, which are major obstacles to the practical application of existing AI systems. Therefore, highly efficient and accurate multimodal search techniques can be very useful for real-time decision support in clinical settings [1, 4].

In this work, we specifically address the most commonly studied image-to-text cross-modal retrieval problem, namely cross-modal

hashing retrieval (hereafter referred to as CMHR). It maps data across different modalities into the same Hamming space, which enables efficient similarity-based retrieval. Hashing-based retrieval methods have significant advantages in terms of memory efficiency and computational speed, making them particularly suitable for clinical environments where real-time processing is required. Existing CMHR techniques can be broadly categorized into the following based on their training methods: Shallow methods, Deep hashing methods, Semi-deep methods. Most of the existing research emphasizes on speed and storage efficiency, which leads to an imbalance problem with accuracy [10, 31, 32].

To address these issues, various attempts have been made in recent years to improve accuracy. For example, Modality-specific Projection Learning, Semantic Consistency Preservation, and Modality-invariant Hash Code Learning via Adversarial Training have been introduced [33, 37, 38]. However, they often come with drawbacks such as increased model complexity and poor generalization ability.

Recently, CLIP-based models have gained attention for their strong cross-modal representation learning performance in general domains. In particular, domain-specific pre-trained models, such as BiomedCLIP, are good at semantic mapping between medical images and medical documents, and show strong performance even in a zero-shot setting. In this regard, CLIP-based models are highly advantageous to be utilized as the backbone of CMHR. Several approaches have been explored in prior work, including UCMFH, DScPH and DDBH [7–9, 14, 17, 19, 26–28, 34, 39].

However, existing CLIP-based CMHR methodologies mostly follow a modality-specific separation structure, and there is a lack of research with explicit fusion structures. In contrast, in the general multimodal learning field, various fusion structures (e.g., Attention-based, Transformer-based, etc.) are used and have shown good performance [3, 11, 15, 24, 25].

The first study to introduce the Fusion module in CMHR is UCMFH [34]. In this study, we propose a novel fusion module by integrating several methodological advances, aiming to enhance performance. More specifically, a novel form of fusion strategy that combines Dropout Voting and MoE are included to improve the performance of CMHR in the medical field [22, 23, 25]. The proposed structure focuses on improving accuracy while maintaining the speed and memory efficiency of hashing techniques, and shows promise in real-world clinical settings. Our main methodological contributions are as follows.

- MoE Fusion Transformer: For the first time, to the best of our knowledge, we have applied the Fusion Module

*Both authors contributed equally to this research.

† Corresponding author.

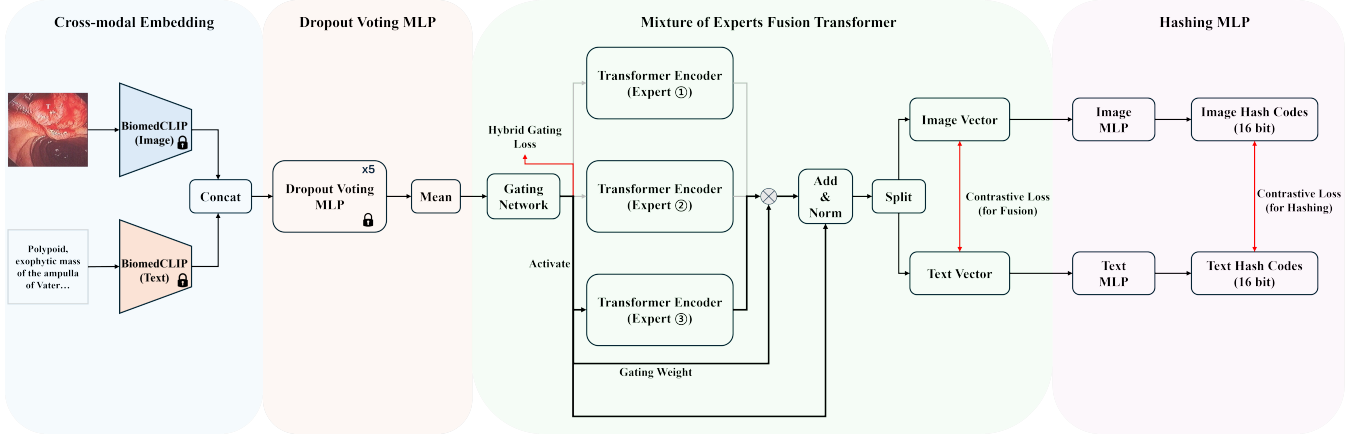


Figure 1: The overview of our proposed model MCMFH.

with MoE structure to CMHR. A MoE transformer strengthens image–text fusion under the low memory budget, improving robustness on both radiology and non-radiology datasets.

- **Frozen Dropout Voting:** A stochastic voting module perturbs input features extracted from the CLIP backbone and averages them, acting as a representation-level ensemble that boosts generalization without extra trainable parameters.
- **Hybrid Gating Loss:** We introduce a task + load-balancing hybrid loss that regularizes the MoE gate and yields the best average performance across datasets.

2 Method

In this section, we will describe the proposed MCMFH model. The overall model structure can be seen in figure 1.

2.1 Cross-modal Embedding

To provide medical-domain-aware multi-modal features, we adopt not the original CLIP models optimized for general domains (e.g., web image-caption pairs) but BiomedCLIP [36]. Trained on millions of paired medical images and reports, BiomedCLIP captures lesion cues and specialized medical terminology that standard CLIP encoders overlook. BiomedCLIP maps each medical image (x_{image}) and its medical description (x_{text}) into 512-dimensional embeddings, and we concatenate the vectors of these two modalities as input to a downstream model. This pre-training based medical multi-modal embedding serves as an important preprocessing step, ensuring that the hashing module is optimized for retrieval while preserving domain-specific semantics.

$$z = \text{Concat} [\text{BiomedCLIP}(x_{\text{image}}), \text{BiomedCLIP}(x_{\text{text}})] \quad (1)$$

2.2 Dropout Voting MLP

We prepend a two-layer MLP in front of the MoE gate.

$$f(z) = W_2 \sigma (\text{Dropout}_{0.2}(W_1 z)), \quad \sigma = \text{GELU} \quad (2)$$

The weights W_1, W_2 are frozen and dropout ($p = 0.2$) is kept active during both training and inference. For each sample we draw ($K = 5$)

independent dropout masks.

$$z_k = f^{(k)}(z), \quad k = 1 \dots K, \quad x = \frac{1}{K} \sum_{k=1}^K z_k, \quad (3)$$

and forward the averaged feature x to the MoE Fusion Transformer (2.3). The effect on the Dropout Voting MLP is as follows. To enhance the robustness of the representation, we apply the dropout multiple times (K) and average the resulting K embeddings. This stochastic ensembling process suppresses noise and reinforces consistent signals aligned with the ground truth, leading to representations that are more likely to reside near the correct class; perturbation-induced correction [12]. Each forward pass activates different sub-networks, enabling the model to learn over a neighborhood rather than a single point in representation space, which improves generalization and reduces overfitting. Additionally, the Voting MLP remains frozen during training, preventing the backbone from adapting to fixed dropout-induced perturbations, thus maintaining a consistent regularization effect [35]. The resulting variance from dropout also encourages the gating network to generate broader routing distributions, mitigating expert collapse, and promoting balanced expert utilization.

2.3 MoE Fusion Transformer

2.3.1 MoE Structure. The MoE Fusion Transformer consists of three main components.

Gating Network. For an input vector x , the gating network computes the selection probability of each expert via softmax.

$$g(x) = \text{softmax}(W_{\text{gate}}x) \quad (4)$$

Only the top-1 expert with the highest probability is then activated, and the rest of the experts are ignored [5].

Experts (Transformer Encoder). Each expert has two layers: a transformer encoder layer with a hidden dimension of 1024 and a self-attention based representation learning with four multi-head attention [30, 34].

Mixture Output & Residual Normalization. The output of the selected expert is multiplied by the selection probability of that expert, which

reflects the confidence of the gating.

$$h(x) = g(x) \cdot \text{Expert}(x) \quad (5)$$

We then applied a residual connection with input x and layer normalization.

$$z = \text{LayerNorm}(h(x) + x) \quad (6)$$

This structure allows the model to extract information from the perspectives of different experts on the same input and dynamically select the output of the most appropriate expert through a gating network to enhance inter-modal interaction.

2.3.2 Hybrid Gating Loss. MoE Fusion Transformer uses a combination of the following two losses to improve the routing performance of the gating network for overall learning stability.

Switch load-balancing loss. Minimizing ($\mathcal{L}_{\text{switch}}$) aligns the realized traffic (T_i) with the gate distribution (P_i) and discourages any single expert from monopolizing the workload, thereby balancing the MoE [6]. The specific loss function is defined as follows:

$$\mathcal{L}_{\text{switch}} = \lambda N \sum_{i=1}^N T_i P_i, \quad (7)$$

where N is the number of experts, B is the batch size, and $\lambda (= 10^{-2})$ is the weighting factor.

$$T_i = \frac{1}{B} \sum_{n=1}^B r_{n,i}, \quad P_i = \frac{1}{B} \sum_{n=1}^B s_{n,i} \quad (8)$$

$$r_{n,i} = \begin{cases} 1 & \text{if sample } n \text{ is routed to expert } i, \\ 0 & \text{otherwise} \end{cases}$$

$s_{n,i}$ = softmax score for expert i before top-1

Variance-based load-balancing loss. Minimizing the (\mathcal{L}_{var}), we directly reduce the variance of the probability of choosing a particular expert, which prevents the gating network from producing biased probabilities [21]. The specific loss function is defined as follows:

$$\mathcal{L}_{\text{var}} = N \sum_{i=1}^N \left(p_i - \frac{1}{N} \right)^2 \quad (9)$$

Hybrid Gating Loss. We configured it to compute a hybrid loss as a weighted sum of the two losses. This allows the gating network to reduce the bias of the expert selection probability and keep the actual selection distribution uniform, thus ensuring the stability of inter-expert learning.

2.3.3 Fusion Contrastive Learning. The vector z transformed by the MoE Fusion Transformer is split into image vector z^v and text vector z^t in the same order as when it was originally concatenated. We apply the same fusion contrastive loss ($\mathcal{L}_{\text{fusion}}$) used in UCMFH [34] to induce cross-modal alignment. This loss maximizes the similarity between aligned image-text pairs and trains them to be distinct from the rest of the pairs.

2.4 Hashing MLP

Following UCMFH [34], we reuse the same two-layer hashing MLP (ReLU–Dropout–Tanh) and *sign* quantization to map the fused image and text features to hash codes. The subsequent hash contrastive loss ($\mathcal{L}_{\text{hash}}$) is identical to that work, so we refer readers to UCMFH for implementation details.

2.5 Overall Objective Function

The overall objective function is organized as follows. The weighting values for each element were specified through experimentation.

$$\mathcal{L} = \mathcal{L}_{\text{fusion}} + 0.85 \cdot \mathcal{L}_{\text{switch}} + 0.15 \cdot \mathcal{L}_{\text{var}} + 0.5 \cdot \mathcal{L}_{\text{hash}} \quad (10)$$

3 Experiments

3.1 Datasets and Metrics

As a dataset to demonstrate the effectiveness of our methodology, we used the open-i data, which is one of the frequently used radiology data in the field of medical vision. [29] Meanwhile, for non-radiology data, we used the non-radiology sub-dataset of the ROCO dataset. [16]

- *Open-i:* There are a total of 121 problem types. Rare problems with less than 20 occurrences were not utilized, and only half of ‘normal’ problems with the most occurrences were kept to reduce class imbalance. Finally, we removed problems that do not correspond to diseases, such as ‘Medical Device’ and ‘No Indexing’ problems, and used 39 types in total.
- *ROCO/Non-Radiological:* ROCO is a multimodal medical image-to-text dataset that provides medical images collected from articles in PubMed Central, along with captions, labels (UMLS semantic types), and section information. [2] We used the top 10 types of occurrences based on semantic types.

In both datasets, we extracted label data based on one-hot encoding. In addition, the ratio of query: retrieval: train data was 1:6:3. To evaluate retrieval performance, we use mean Average Precision (mAP), the standard metric in CMHR, for both image-to-text (I2T) and text-to-image (T2I) tasks. Following UCMFH [34], we compute mAP exactly as specified in their protocol.

3.2 Experimental Setup

The main hyperparameters were set as follows: the batch size was 32, and the number of training epochs was 150. The learning rate was set to 0.0001 for the MoE Fusion Transformer and 0.001 for both the image and text branches of the Hashing MLP. The hash code length was primarily fixed to 16 bits, as our focus was on achieving high retrieval performance with reduced memory usage, which is crucial for practical applications in the medical domain. The Adam [13] optimizer was employed for all training components.

3.3 Performance

To prove its effectiveness in terms of clinical practicality, we compared the retrieval performance based on 16 bit hash code, which is low memory. In addition, as our methodology is CLIP Based, we compared UCMFH [34] with two additional most recent CLIP Based

Table 1: Comparative Analysis of Baselines, Proposed Model, and Ablation Variants based on mAP

Exp.	Method \ Dataset	open-i			roco/non-rad		
		I2T-16 (32/64)	T2I-16 (32/64)	Mean-16 (32/64)	I2T-16 (32/64)	T2I-16 (32/64)	Mean-16 (32/64)
Main Comp.	DScPH	.194(.247/.280)	.186(.208/.235)	.190(.227/.257)	.526(.525/.551)	.516(.516/.520)	.521(.520/.535)
	DDBH	.401(.432/.449)	.297(.299/.318)	.349(.366/.384)	.564(.598/.600)	.538(.565/.566)	.551(.582/.583)
	UCMFH	.354(.367/.382)	.371(.375/.391)	.362(.373/.386)	.634(.657/.646)	.653(.661/.659)	.643(.659/.652)
	MCMFH(Ours)	.429(.436/.434)	.423(.429/.434)	.426(.432/.434)	.687(.662/.665)	.699(.652/.674)	.693(.657/.669)
Module Abl.	Base(UCMFH)	.354	.371	.362	.634	.653	.643
	+MoE	.412	.412	.412	.655	.628	.641
	+MoE+Voting1+Frozen	.383	.381	.382	.645	.651	.648
	+MoE+Voting5+Unfrozen	.404	.395	.399	.650	.649	.649
	+MoE+Voting5+Frozen(Ours)	.429	.423	.426	.687	.699	.693
Loss Abl.	MCMFH w/Switch	.421	.410	.416	.680	.693	.687
	MCMFH w/Variance-based	.419	.418	.419	.682	.685	.684
	MCMFH w/Hybrid	.429	.423	.426	.687	.699	.693

CMHR models: DScPH [20], DDBH [18]. For a fair comparison, we unified the backbone CLIP model to bioMedCLIP and matched the hyperparameters such as epoch, batch size, and random seed. Despite DScPH and DDBH training up to the CLIP backbone, the results in Table 1 show that our model’s mAP is larger than DScPH by 0.236 in open-i and 0.172 in roco/non-rad, and our model is larger than DDBH by 0.077 in open-i and 0.142 in roco/non-rad. We can also see that our methodology is more efficient in terms of both resources required for training and performance since we do not train CLIP itself.

Finally, we can see that the average mAP value is 0.064 larger in open-i and 0.05 larger in roco/non-rad than UCMFH, which performs rather well compared to other modern models. Additional 32 bit and 64 bit experiments also showed mostly improved performance. (Table 1) This confirmed the practicality of our model, which performed well at the lowest 16 bits.

3.4 Ablation Study

3.4.1 Effect of MoE. Table 1 shows the effectiveness of one of our key ideas, the MoE Fusion Transformer. In particular, for open-i, we can see that it leads to a significant increase in the resulting average mAP of 0.05. For roco/non-rad, we can see that the combination of MoE and Frozen Dropout Voting MLP with expert balancing works well.

3.4.2 Effect of Dropout Voting MLP. The effect of Frozen on the Dropout Voting MLP can also be seen from the results of the Table 1 experiment. First, we can see the effect of Frozen in maximizing the dropout effect, as the average mAP value is 0.027 higher in open-i and 0.044 higher in roco/non-rad. Finally, the effect of voting can also be seen as the average mAP value is 0.044 larger in open-i and 0.045 larger in roco/non-rad when the number of votes is 5 than when the number of votes is 1. Taken together, these results show that the features input to the MoE Fusion Transformer after the Frozen Dropout Voting MLP are transformed into more generalized

and stable features, which in turn leads to better performance of the overall model.

3.4.3 Effect of Hybrid Gating Loss. Table 1 shows that the hybrid loss in the final architecture has the best mAP in the entire dataset. This shows that the hybrid loss aligns the selection probability with the actual expert selection rate through the switch loss, and minimizes the variance through the variance loss. This further equalizes the selection probability and contributes to achieving stable performance improvement.

3.4.4 Retrieval Efficiency. Finally, to verify clinical practicality, we compared retrieval latency between 16 bit hash codes and real-valued features. On average across the two datasets, real-valued retrieval was 1.73 times slower. It is also 1/4 more memory efficient than 64 bit, which increases its practicality in terms of speed and memory efficiency.

4 Conclusion

In this paper, we propose MCMFH on the CMHR task and take a step towards its practicality in the clinical environment by demonstrating the balancing effectiveness of MCMFH in the medical domain, which satisfies both resource efficiency and mAP performance. As shown in the experimental results, MCMFH outperforms the existing baseline and recent CLIP-based CMHR methods, DScPH and DDBH, in both I2T and T2I at a lower bit count of 16 bits. Future work will extend beyond cross-modal retrieval to evaluate the effectiveness of the proposed approach in environments involving three or more modalities, using larger and more diverse medical datasets.

GenAI Usage Disclosure

Generative AI tools were used exclusively for minor editing, grammar correction, and providing ideas specifically for the outline of the manuscript, as well as for translating portions of the text. All scientific content, analysis, and interpretation are entirely the original work of the authors.

References

- [1] Julián N Acosta, Guido J Falcone, Pranav Rajpurkar, and Eric J Topol. 2022. Multimodal biomedical AI. *Nature medicine* 28, 9 (2022), 1773–1784.
- [2] Olivier Bodenreider. 2004. The Unified Medical Language System (UMLS): integrating biomedical terminology. *Nucleic Acids Research* 32, suppl_1 (2004), D267–D270. doi:10.1093/nar/gkh061
- [3] Yen-Chun Chen, Linjie Li, Licheng Yu, Ahmed El Kholy, Faisal Ahmed, Zhe Gan, Yu Cheng, and Jingjing Liu. 2020. UNITER: UNiversal Image-Text Representation Learning. In *European Conference on Computer Vision (ECCV)*.
- [4] Andre Esteva, Alexandre Robicquet, Bharath Ramsundar, Volodymyr Kuleshov, Mark DePristo, Katherine Chou, Claire Cui, Greg Corrado, Sebastian Thrun, and Jeff Dean. 2019. A guide to deep learning in healthcare. *Nature medicine* 25, 1 (2019), 24–29.
- [5] William Fedus, Jeff Dean, and Barret Zoph. 2022. A review of sparse expert models in deep learning. *arXiv preprint arXiv:2209.01667* (2022).
- [6] William Fedus, Barret Zoph, and Noam Shazeer. 2022. Switch transformers: Scaling to trillion parameter models with simple and efficient sparsity. *Journal of Machine Learning Research* 23, 120 (2022), 1–39.
- [7] Yadong Huo, Qin Qibing, Jiangyan Dai, Wenfeng Zhang, Lei Huang, and Chengduan Wang. 2024. Deep neighborhood-aware proxy hashing with uniform distribution constraint for cross-modal retrieval. *ACM Transactions on Multimedia Computing, Communications and Applications* 20, 6 (2024), 1–23.
- [8] Yadong Huo, Qibing Qin, Jiangyan Dai, Lei Wang, Wenfeng Zhang, Lei Huang, and Chengduan Wang. 2023. Deep semantic-aware proxy hashing for multi-label cross-modal retrieval. *IEEE Transactions on Circuits and Systems for Video Technology* 34, 1 (2023), 576–589.
- [9] Yadong Huo, Qibing Qin, Wenfeng Zhang, Lei Huang, and Jie Nie. 2024. Deep hierarchy-aware proxy hashing with self-paced learning for cross-modal retrieval. *IEEE Transactions on Knowledge and Data Engineering* (2024).
- [10] Qing-Yuan Jiang and Wu-Jun Li. 2017. Deep cross-modal hashing. In *Proceedings of the IEEE conference on computer vision and pattern recognition*. 3232–3240.
- [11] Douwe Kiela, Jannis Bulian, Christos Baziotis, Hamed Firooz, John Giorgi, Zhiguo Jin, Arjun Mohan, and et al. 2019. Supervised Multimodal Bitransformers for Classifying Images and Text. In *Proceedings of the 2019 Conference on Empirical Methods in Natural Language Processing (EMNLP)*.
- [12] Dongwon Kim, Namyup Kim, and Suha Kwak. 2023. Improving cross-modal retrieval with set of diverse embeddings. In *Proceedings of the IEEE/CVF conference on computer vision and pattern recognition*. 23422–23431.
- [13] Diederik P Kingma. 2014. Adam: A method for stochastic optimization. *arXiv preprint arXiv:1412.6980* (2014).
- [14] Yishu Liu, Qingpeng Wu, Zheng Zhang, Jingyi Zhang, and Guangming Lu. 2023. Multi-granularity interactive transformer hashing for cross-modal retrieval. In *Proceedings of the 31st ACM International Conference on Multimedia*. 893–902.
- [15] Jiaseen Lu, Dhruv Batra, Devi Parikh, and Stefan Lee. 2019. ViLBERT: Pretraining Task-Agnostic Visiolinguistic Representations for Vision-and-Language Tasks. In *Advances in Neural Information Processing Systems (NeurIPS)*.
- [16] Obioma Pelka, Sven Koitka, Johannes Rückert, Felix Nensa, and Christoph M. Friedrich. 2018. Radiology Objects in COntext (ROCO): A Multimodal Image Dataset. In *Intravascular Imaging and Computer Assisted Stenting and Large-Scale Annotation of Biomedical Data and Expert Label Synthesis (Lecture Notes in Computer Science, Vol. 11043)*. Springer, 180–189. doi:10.1007/978-3-030-01364-6_20
- [17] Qibing Qin, Yadong Huo, Wenfeng Zhang, Lei Huang, and Jie Nie. 2025. Deep Discriminative Boundary Hashing for Cross-modal Retrieval. *IEEE Transactions on Circuits and Systems for Video Technology* (2025).
- [18] Qibing Qin, Yadong Huo, Wenfeng Zhang, Lei Huang, and Jie Nie. 2025. Deep Discriminative Boundary Hashing for Cross-modal Retrieval. *IEEE Transactions on Circuits and Systems for Video Technology* (2025), 1–1. doi:10.1109/TCSVT.2025.3570128
- [19] Qibing Qin, Lei Wu, Wenfeng Zhang, Lei Huang, and Jie Nie. 2025. Deep Semantic-consistent Penalizing Hashing for Cross-modal Retrieval. *IEEE Transactions on Multimedia* (2025).
- [20] Qibing Qin, Lei Wu, Wenfeng Zhang, Lei Huang, and Jie Nie. 2025. Deep Semantic-consistent Penalizing Hashing for Cross-modal Retrieval. *IEEE Transactions on Multimedia* (2025), 1–14. doi:10.1109/TMM.2025.3535306
- [21] Noam Shazeer, Azalia Mirhoseini, Krzysztof Maziarz, Andy Davis, Quoc Le, Geoffrey Hinton, and Jeff Dean. 2017. Outrageously large neural networks: The sparsely-gated mixture-of-experts layer. *arXiv preprint arXiv:1701.06538* (2017).
- [22] Noam Shazeer, Azalia Mirhoseini, Krzysztof Maziarz, Andy Davis, Quoc V Le, Geoffrey Hinton, and Jeff Dean. 2017. Outrageously Large Neural Networks: The Sparsely-Gated Mixture-of-Experts Layer. In *International Conference on Learning Representations (ICLR)*.
- [23] Nitish Srivastava, Geoffrey Hinton, Alex Krizhevsky, Ilya Sutskever, and Ruslan Salakhutdinov. 2014. Dropout: A Simple Way to Prevent Neural Networks from Overfitting. *Journal of Machine Learning Research* 15, 1 (2014), 1929–1958.
- [24] Hao Tan and Mohit Bansal. 2019. LXMERT: Learning Cross-Modality Encoder Representations from Transformers. In *Proceedings of the 2019 Conference on Empirical Methods in Natural Language Processing (EMNLP)*.
- [25] Yao-Hung Hubert Tsai, Shaojie Bai, Paul Pu Liang Yamada, Louis-Philippe Morency, and Ruslan Salakhutdinov. 2019. Multimodal Transformer for Unaligned Multimodal Language Sequences. In *Proceedings of the Annual Meeting of the Association for Computational Linguistics (ACL)*.
- [26] Junfeng Tu, Xueliang Liu, Yanbin Hao, Richang Hong, and Meng Wang. 2024. Two-step discrete hashing for cross-modal retrieval. *IEEE Transactions on Multimedia* (2024).
- [27] Junfeng Tu, Xueliang Liu, Zhen Huang, Yanbin Hao, Richang Hong, and Meng Wang. 2025. Cross-modal Hashing via Diverse Instances Matching. *IEEE Transactions on Image Processing* (2025).
- [28] Junfeng Tu, Xueliang Liu, Zongxiang Lin, Richang Hong, and Meng Wang. 2022. Differentiable cross-modal hashing via multimodal transformers. In *Proceedings of the 30th ACM International Conference on Multimedia*. 453–461.
- [29] U.S. National Library of Medicine. 2013. Open-I: An Open Access Biomedical Image Search Engine. <https://openi.nlm.nih.gov>. Accessed: 2025-06-07.
- [30] Ashish Vaswani, Noam Shazeer, Niki Parmar, Jakob Uszkoreit, Llion Jones, Aidan N Gomez, Lukasz Kaiser, and Illia Polosukhin. 2017. Attention is all you need. *Advances in neural information processing systems* 30 (2017).
- [31] Jingdong Wang, Ting Zhang, Nicu Sebe, Heng Tao Shen, et al. 2017. A survey on learning to hash. *IEEE transactions on pattern analysis and machine intelligence* 40, 4 (2017), 769–790.
- [32] Tianshi Wang, Fengling Li, Lei Zhu, Jingjing Li, Zheng Zhang, and Heng Tao Shen. 2025. Cross-modal retrieval: a systematic review of methods and future directions. *Proc. IEEE* (2025).
- [33] Fei Wu, Xiao-Yuan Jing, Zhiyong Wu, Yimu Ji, Xiwei Dong, Xiaokai Luo, Qinghua Huang, and Ruchuan Wang. 2020. Modality-specific and shared generative adversarial network for cross-modal retrieval. *Pattern Recognition* 104 (2020), 107335.
- [34] Xinyu Xia, Guohua Dong, Fengling Li, Lei Zhu, and Xiaomin Ying. 2023. When CLIP meets cross-modal hashing retrieval: A new strong baseline. *Information Fusion* 100 (2023), 101968. doi:10.1016/j.inffus.2023.101968
- [35] Fan Zhang, Xian-Sheng Hua, Chong Chen, and Xiao Luo. 2024. Fine-grained Prototypical Voting with Heterogeneous Mixup for Semi-supervised 2D-3D Cross-modal Retrieval. In *Proceedings of the IEEE/CVF Conference on Computer Vision and Pattern Recognition*. 17016–17026.
- [36] Sheng Zhang, Yanbo Xu, Naoto Usuyama, Hanwen Xu, Jaspreet Bagga, Robert Tinn, Sam Preston, Rajesh Rao, Mu Wei, Naveen Valluri, et al. 2023. Biomed-clip: a multimodal biomedical foundation model pretrained from fifteen million scientific image-text pairs. *arXiv preprint arXiv:2303.00915* (2023).
- [37] Ying Zhang and Huchuan Lu. 2018. Deep cross-modal projection learning for image-text matching. In *Proceedings of the European conference on computer vision (ECCV)*. 686–701.
- [38] Liangli Zhen, Peng Hu, Xu Wang, and Dezhong Peng. 2019. Deep supervised cross-modal retrieval. In *Proceedings of the IEEE/CVF conference on computer vision and pattern recognition*. 10394–10403.
- [39] Congcong Zhu, Qibing Qin, Wenfeng Zhang, and Lei Huang. 2025. Deep neighbor-coherence hashing with discriminative sample mining for supervised cross-modal retrieval. *Expert Systems with Applications* 279 (2025), 127365.